Theor Chim Acta (1986) 69: 393-407

Theoretica Chimica Acta

Wavefunction comparisons for the valence-bond model for conjugated π-networks*

D. J. Klein, S. A. Alexander, W. A. Seitz, T. G. Schmalz, and G. E. Hite

Theoretical Chemical Physics Group, Department of Marine Sciences, Texas A and M University at Galveston, Galveston, TX 77553-1675, USA

(Received August 26, 1985/Accepted January 6, 1986)

Approximate ground-state wavefunctions for valence-bond (or Heisenberg) models are obtained both within Néel-state-based and within Kekulé-state-based resonance-theoretic approaches. Comparisons are made between these and other general approaches, with particular emphasis on organic π-network systems. Attention is drawn to the manner in which the quality of the different approximation schemes changes with variations in structural characteristics of the system. It is suggested that resonance-theoretic ideas are most appropriate for (aromatic benzenoid) systems with low coordination number, whereas Néel-state based ideas are most appropriate for (3-dimensional) structures with higher coordination number (and little "frustration").

Key words: Valence-bond model — π-Networks — Heisenberg model — Resonance theory — Néel states — Renormalization group — Spin waves

1. Introduction

Though the valence-bond (VB) model [1] for conjugated π-networks was introduced in the 1930's, subsequently criticisms were advanced that have plagued the model's use to the present day. For instance, the difficulty of suggested solutions (essentially via configuration interaction) was found to increase exceedingly rapidly with system size, typically even if one restricts matrix diagonalization to the resonance-theoretic subspace of Kekulé structures. In solid-state physics [2] the Heisenberg model for cooperative magnetism was developed and there

* Work supported by The Robert A. Welch Foundation of Houston, Texas

too criticisms were advanced, though they did not seriously hinder the model's use and, in particular, seemingly successful methods of solution were found [2, 3]. But the simple VB model is formally identical to the Heisenberg model (for the antiferromagnetically-signed isotropic spin-$\frac{1}{2}$ case). Thus the differing degrees of success of the Néel-state-based and resonance-theoretic approaches, used respectively by physicists and chemists, might be surmised to indicate a serious difficulty in the latter approach. Further support for the view that the two approaches are inconsistent might be seen in the associated contrasting long-range orderings: for Néel-state-based approaches, a long-range alignment of spin orientations; and for Kekulé-structure-based approaches, only a short-range ordering of spin-alignments, although at least in some circumstances for the resonance-theoretic case another (competing) type of long-range order is exhibited [4–6].

Here we investigate these two types of approximation schemes. Particular emphasis is placed upon structures with lower (mean) coordination numbers, such as is characteristic of organic π-network systems. In fact the Néel-state-based approaches are rather poorly studied for such systems since these approaches have usually been applied to inorganic antiferromagnets which typically involve 3-dimensional structures of relatively high coordination number. On the other hand resonance-theoretic studies seem to have been limited to small finite systems. Most of the usual [2, 3] mean-field approaches of solid-state physics reduce at zero-temperature to a single Néel state, and so make common ground-state comparisons. An oft-espoused antiferromagnetic spin-wave extension [2, 7] is also compared, as well as the singlet spin projection of the Néel state and a second-order perturbation correction [8] to the Néel-state result. For the Kekulé-state based viewpoint, in addition to the simple resonance theory [1] wavefunction *ansatz* we consider the even more primitive basis states consisting of single Kekulé structures. In seeking an accurate estimate of the exact ground-state energy for the graphite lattice so as to more fully gauge the reliability of these various approximations we include all available variational upper bounds, most of which are developed in the appendices.

For the numerical work we utilize the simple nearest-neighbor VB model Hamiltonian

$$H = 2J \sum_{i\sim j}^{\Gamma} \boldsymbol{s}_i \cdot \boldsymbol{s}_j \tag{1}$$

where the sum is over nearest-neighbor pairs of sites of the *molecular graph* Γ, $\boldsymbol{s}_k$ is the spin operator for site k, and $J>0$ is the *exchange* parameter. Generally, the *Néel states* we consider will be restricted to *alternant* (or bipartite) graphs Γ, for which the sites may be partitioned into two sets A and B such that sites of one set are nearest neighbors only to sites in the other set. The *standard* Néel state then is [2, 3]

$$|0\rangle = \prod_{i\in A} \alpha(i) \prod_{j\in B} \beta(j), \tag{2}$$

where $\alpha(k)$ and $\beta(k)$ represent the spin-up and spin-down states for site k. A

typical (unnormalized) *Kekulé state* is

$$|K\rangle = \prod_{i\sim j}^{K} \{\alpha(i)\beta(j) - \beta(i)\alpha(j)\}, \tag{3}$$

where the product is over a set K of disjoint edges of Γ such that every site is covered. For alternant Γ it is convenient to choose the indices i of Eq. (3) to be in A. Though Kekulé states may be defined on some non-alternant graphs, when Γ is alternant a necessary (but not sufficient) condition that such states exist is that A and B have the same numbers of sites.

2. General comparisons

First, standard matrix element techniques readily yield energies of single Kekulé and Néel states

$$\begin{aligned} &\langle K|H|K\rangle/\langle K|K\rangle = -\tfrac{3}{4}JN \\ &\langle 0|H|0\rangle = -\tfrac{1}{4}zJN, \end{aligned} \tag{4}$$

where N is the number of sites and z is the mean *coordination number* of Γ (so that zN is the number of edges of Γ). From the plot of these energies in Fig. 1 we see that the Kekulé state energy is lower in the low ($z \leq 3$) coordination number region whereas the Néel-state energy is lower in the high ($z \geq 3$) region.

Pauling and Wheland's resonance theory [1, 9] often improves upon the single Kekulé-structure energy. In this approach a simple sum over the different possible (global) Kekulé structures is taken. To indicate an example of this improvement we then also plot in Fig. 1 an optimal resonance energy result (obtained from the minimum energy on the interpolated continuous $\Delta\varepsilon/J$ vs. Q/w curves of [5]

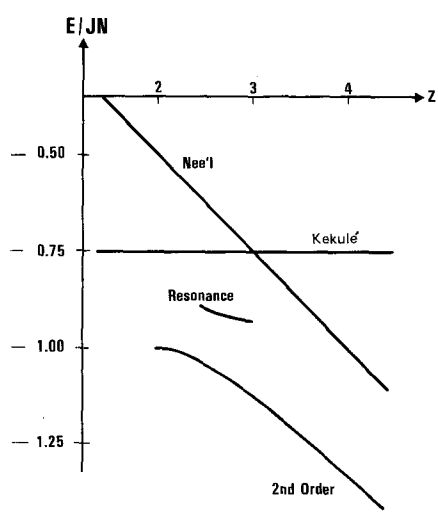

Fig. 1. Comparison of energy estimates for the Heisenberg model on various representative graphs as a function of mean coordination number z

where calculations are performed for extended poly-polyphenanthrene fusenes). However, the resonance-energy result does not always yield a significant improvement over the energy per site of a single Kekulé structure even if there is more than one such structure. A lowering of the energy can only be obtained by admixing structures which differ only locally (i.e., at a few nearby sites) from a typical Kekulé structure. (Otherwise the Hamiltonian matrix element connecting the structures will be vanishingly small.) The admixed structures can be viewed as being generated by local modifications of the reference structure which occur *independently* of distant regions of the structure. If the number of such local modifications to a typical Kekulé structure is size-extensive (i.e., scales $\sim N$), then a nonzero improvement to the energy per site is expected. But also in this case, if the modification occurs independently as stipulated, the number $\#_N$ of structures should scale exponentially with N. Thus the importance of Kekulé structures for size-extensive properties is expected [6, 10] to scale as the ratio

$$\rho = \frac{\ln \#_N}{N}. \tag{5}$$

Thence, the utility of Kekulé structures should be greatest if ρ is suitably large. For certain conjugated hydrocarbons this criterion is not met: for instance, the poly-polyacenes [6] for which ρ approaches zero as their strip lengths increase, so that their resonance stabilization (per site) also approaches zero.

In an analogy to resonance theory, one might take a similar equi-weight "sum" over all Néel-type states, with opposing spins on the A and B sets (or sublattices). Since all such Néel states can be obtained upon application of a spin-space rotation $R(\boldsymbol{\omega})$ to $|0\rangle$, the "sum" becomes continuous to give

$$|\Phi\rangle \equiv \frac{1}{8\pi^2} \int d\boldsymbol{\omega}\, R(\boldsymbol{\omega})|0\rangle. \tag{6}$$

In fact this projects out the overall singlet spin component of $|0\rangle$, so $|\Phi\rangle$ is nonzero only if the number of A and B sites are equal (whence also the ground state is known [11] to be a singlet). But as shown in Appendix A this leads to an energy

$$E(\Phi) = \frac{\langle\Phi|H|\Phi\rangle}{\langle\Phi|\Phi\rangle} = -z\left(\frac{1}{4}+\frac{1}{N}\right)JN, \tag{7}$$

so that there is no size-extensive improvement. In fact, regardless of the particular projection taken, there should [12] be no improvement over the per-site energy of a single Néel state for a general alternant Γ.

One might seek to improve the Néel state result via a suitable perturbation-theoretic expansion [8]. Conveniently the (antiferromagnetically-signed) Ising model is taken as the zero-order Hamiltonian

$$H^0 = 2J \sum_{i\sim j}^{\Gamma} s_i^z s_j^z \tag{8}$$

since it has $|0\rangle$ as its ground-state (which is nondegenerate for finite connected Γ, and $J>0$). Through second-order the ground-state energy, for Γ with all sites of the same (integer) coordination number, is [8]

$$E_2 = -\frac{1}{4}\frac{z^2}{z-1}JN. \tag{9}$$

When more than one coordination number occurs, E_2 depends [8] upon further details of Γ, but in Fig. 1 we have plotted the function of (9) as a generic estimate for E_2. As often occurs with second-order estimates, this result presumably is lower than the true ground-state energy. It is seen that the energy correction is largest for smaller z, so that again the Néel state picture is indicated to be less accurate in the region of small z.

3. Specific systems

An example providing further evidence is that of a single cycle. For purposes of comparison we plot in Fig. 2 various energy estimates as a function of (even) cycle-size N. These plotted results are (in order of occurrence in the figure) for:

(a) a single Néel state with energy as in (4);
(b) a single Kekulé state with energy as in (4);
(c) the singlet spin projected Néel state result of (6);
(d) the resonance theory result;
(e) the exact result, obtained numerically via [13, 14] configuration interaction for $N \leq 22$;
(f) a standard [7] nonvariational antiferromagnetic spin-wave result; and
(g) the second-order perturbation-theoretic correction of (9) to the Néel-state picture.

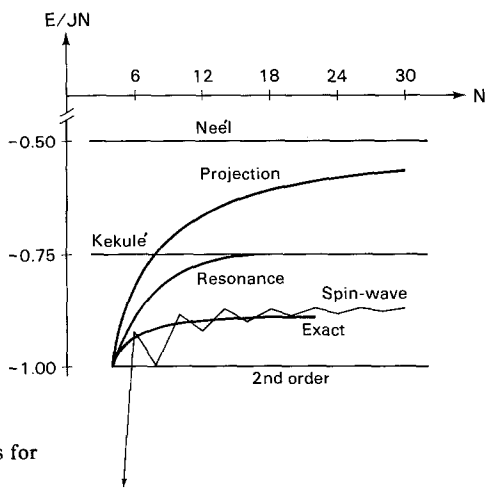

Fig. 2. Comparisons of various energy estimates for a cyclic ring as a function of its (even) size

For this cyclic chain there are just two Kekulé structures, for whch the resonance-theory energy is evaluated to be

$$E_{RT} = -\frac{3}{4}\left(\frac{2^{N/2}+4}{2^{N/2}+2}\right)JN, \tag{10}$$

so that no size extensive correction to the energy for a single Kekulé structure is obtained as $N \to \infty$. This is in agreeent with the vanishing of the ratio $\rho = \ln 2/N$, as $N \to \infty$. But for small N where ρ is larger there is seen to be notable improvement. Similar comments apply to the singlet-spin projected Néel state, though typically the resonance theory result is better. The perturbative Néel-state-based result improves upon a single Néel state, but has an oppositely-signed error of roughly the same size as that of the simple resonance theory. Finally the standard antiferromagnetic spin-wave result, as described in Appendix B, apparently compares quite favorably with the exact results but merits special comment. In fact this Néel-state-based approach, which proceeds via transformation to Boson operators, has [7, 15] serious defects: first, the Hamiltonian is expanded in powers of Boson creation and annihilation operators followed by truncation to just quadratic (and scalar) terms; and second, nonphysical spaces, corresponding to fictitious higher Boson-occupancies are admixed. Marshall [15] is especially critical; he notes the unphysical states are very strongly admixed, as is clearly indicated in that the sublattice magnetization (per site) for cyclic chains is calculated to be (unphysically) infinite. It seems that the reasonable energy estimate is an accidental artifact of several non-validated approximations. For square-planar and cubic lattices (or higher-spin Heisenberg models) Marshall's criticisms [15] tend toward lesser severity. One approach [16] to rectify the difficulties in the spin-wave result leads to a variational bound that is somewhat more difficult to compute and gives an energy near that of the Kekulé structure.

From the data of Fig. 2 it seems perhaps that the resonance-theoretic wavefunction is superior to the simple Néel-state wavefunction or its projection. As the size of the system is increased the energy for this projection worsens, and as the per-site number of Kekulé structures (as measured by ρ) decreases the resonance-theory worsens too. For the ring (especially as $N \to \infty$) there are [17] many other calculations (some related either to Néel-state ideas or to resonance theory); but, they are passed over here, because their increased complexity is sufficient to have (so far) prevented their application to more complicated systems.

The case of graphite is of special interest, in that this achieves the largest coordination number ($z = 3$) possible for conjugated hydrocarbons. Further, our emerging view suggests that larger z provides a more severe test of resonance-theory (compared with Néel-state ideas). For graphite there seem to be few variational bounds that have previously been implemented for the VB model, and in particular the exact answer is not presently known. One type of bound may be obtained through computations on a lattice fragment that if repeated over and over can exactly cover the lattice. In fact, the energy per site of the lowest singlet state of such a fragment (with an even number of sites) is an upper bound to that for the lattice. This is explained in Appendix D following a

Table 1. Energy estimates for graphite lattice ground-state

Method	E/JN
4-site renormalization	−0.7305
Néel state	−0.7500
Single Kekulé structure	−0.7500
7-site renormalization	−0.8388
Resonance theory bound	−0.9238
Resonance theory estimate	−0.929
Exact bound via benzene fragment	−0.9343
Exact bound via naphthalene fragment	−0.9540
Exact bound via fragment of 4c	−0.9657
Exact bound via fragment of 4d	−0.9719
Exact bound via fragment of 4e	−0.9902
Exact bound via fragment of 4f	−0.998
Antiferromagnetic spin-wave estimate	−1.106
Second-order Néel-state perturbation	−1.125

description in Appendix C of a related renormalization-group approach [18] for lattice fragments of other spin multiplicities. A point of some interest is that these (currently) best upper bounds have the type of long-range order characteristic of resonance-theoretic wavefunctions rather than that of the Néel state. These numerical computations of fragment energies are carried out via an efficient unitary group method [13]. The various graphite energy estimates we obtain are reported in Table 1. It is seen that the first-order renormalization-group upper bounds based upon 4- and 7-site clusters of Fig. 3 are not as good (i.e., as low) as the resonance-theory results. The best upper bounds evidently are obtained for the sequence of spin-singlet fragments of Fig. 4. From these results we estimate the graphite ground-state energy to be roughly midway between the resonance theory results and the second-order Néel-state perturbation result. The antiferromagnetic spin-wave result, though apparently again experiencing a cancellation of errors, we feel is still suspect because of the general defects mentioned earlier.

Yet another system providing evidence is found in the work of Anderson and Fazekas [19] on the triangular-lattice (spin-$\frac{1}{2}$) Heisenberg model. Having many 3-cycles this lattice exhibits much frustration, so that the generalized (3-sublattice) Néel state gives an energy that is rather high in comparison with the Néel-state energy on unfrustrated lattices of the same coordination number, $z=6$. In fact,

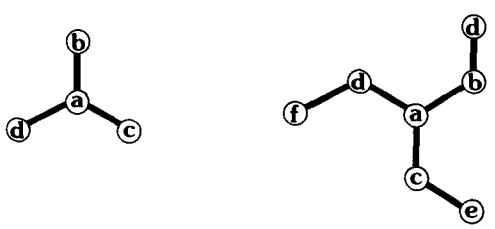

Fig. 3. The 4- and 7-site clusters used in a (near) conventional real-space renormalization group approach

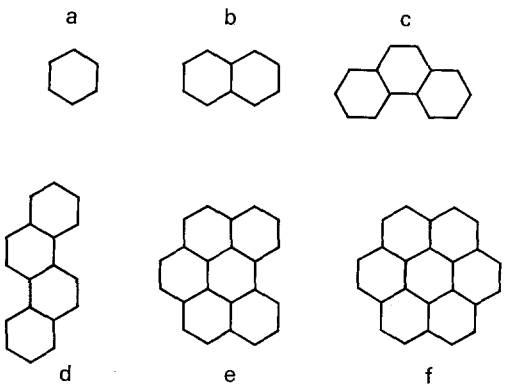

Fig. 4. Six fragments which can cover the graphite lattice as explained in the text. These fragments represent the best upper bounds of systems of a given number of fused rings that we have investigated

this (3-sublattice) Néel-state energy is the same as that of a single Kekulé structure on the triangular lattice, and a resonance-theoretic combination of Kekulé structures should only improve upon this energy. Then in view of evidence, much like that we find for the "borderline" case of graphite, Anderson and Fazekas suggest [19] that the ground state for the case of a triangular lattice is well described as being of the resonance-theoretic type. Their estimates for the energy of the resonance-theory wavefunction could presumably be improved upon using our graph-theoretic methods [5]. Similarly our present upper-bounding methods should make improvements; indeed the 4×4 diamond-shaped fragment from the triangular lattice leads to an upper bound of -0.825767 J for the ground-state energy per site, noticeably surpassing their best value of -0.7432 J. It is of some interest that for the triangular lattice Anderson and Fazekas find evidence for a (different) type of Kekulé-structure-related long-range order.

4. Conclusion

The evidence we have gathered here clarifies the applicability of two contrasting qualitative views of the nature of the ground state of the VB (or spin-$\frac{1}{2}$ Heisenberg) model. Basically it seems that Néel-state and resonance-theoretic descriptions apply best under different (structural) conditions. The suggestions from our evidence may be summarized in two propositions:

I. Resonance-theoretic descriptions are most appropriate for (benzenoid or aromatic [20]) systems with low mean coordination number ($z \lesssim 3$) and with many Kekulé structures per site ($\rho \gtrsim 0.05$).

II. Néel-state-based descriptions are most appropriate for (3-dimensional) structures with high mean coordination numbers and low extents of frustration (i.e., few small odd cycles of antiferromagnetically-signed interactions).

Still the argument from the currently available data is not completely conclusive, in part because of the difficulty in obtaining reliably accurate results for large system solutions. But there remains a (perhaps more persuasive) argument favor-

ing our propositions: first, I is supported by the experimental success of both qualitative [9] and quantitative [1] resonance models in application to benzenoid π-networks (satisfying the conditions of I); and second II is supported by similar experimental successes of Néel-state based theories as applied [3] in the field of cooperative magnetism (to systems satisfying the conditions of II). In fact the parenthetic restrictions to benzenoid [20] systems in I and 3-dimensional systems in II are suggested more from the areas of these experimental successes than from our data in the preceding sections.

Of course, these empirical successes might be more pronounced for more accurate models than for the nearest-neighbor VB model discussed here. In fact, there is some evidence for this in the application to aromatic benzenoids, in that higher-order corrections tend to enhance the Kekulé-structure approaches while detracting from Néel-state approaches. That is, for aromatic benzenoids the next corrections to H of (1) entail [19] next-nearest-neighbor interactions (etc.) that have a sign to "frustrate" Néel-state ordering. Indeed at somewhat high strengths these interactions yield [19] models for which the Kekulé structures are exact (degenerate) ground states. Then in a first-order degenerate perturbation treatment based upon such 0-order models with the perturbation involving the additional nearest-neighbor interaction, one would seek to diagonalize a matrix like that for H of (1) for the restricted subspace of Kekulé structures. But of course this is essentially what has often been done in organic chemistry, though the motivation has often been more empirically based. In solid-state physics also other higher-order corrections sometimes seem to enhance Néel-state descriptions; for instance, anisotropic spin-dependent Ising-type perturbations often occur [3] for transition metals and especially rare earths.

In conclusion it seems that the propositions (I and II) we have advanced might resolve otherwise apparently conflicting views. Further work to separate features of the model from those of the approximate solutions would be useful.

Appendix A: projected Néel state

The wavefunction ansatz of (5) may be rewritten as

$$|\Phi\rangle = \mathcal{O}_0|0\rangle, \tag{A.1}$$

with $\mathcal{O}_0$ the singlet spin projection operator. Because H commutes with $\mathcal{O}_0$, which is idempotent,

$$\langle\Phi|H|\Phi\rangle = \langle 0|H\mathcal{O}_0|0\rangle. \tag{A.2}$$

Now the spin rotations (in $\mathcal{O}_0$) are representable as

$$R(\alpha, \beta, \gamma) = e^{i\alpha S^z}\, e^{i\beta S^y}\, e^{i\gamma S^z}, \tag{A.3}$$

where α, β, γ are Euler angles (ranging over 2π, π, 2π) and where S^μ are components ($\mu = x, y, z$) of the total spin. Then because $|0\rangle$ is an eigenket to S^z

(as well as to $e^{i\gamma S^z}$ and $e^{i\alpha S^z}$, which also commute with H),

$$\langle\Phi|H|\Phi\rangle = \tfrac{1}{2}\int_0^{\pi} \sin\beta\langle 0|H\, e^{i\beta S^y}|0\rangle\, d\beta. \tag{A.4}$$

Next the expression of (1) is used and $e^{i\beta S^y}$ is written as the N-fold product of rotations for the spin of each site,

$$\langle 0|H\, e^{i\beta S^y}|0\rangle = 2J \sum_{p\sim q} \langle 0|\boldsymbol{s}_p \cdot \boldsymbol{s}_q \prod_r e^{i\beta s_r^y}|0\rangle. \tag{A.5}$$

Each single site is of spin-$\frac{1}{2}$ so that the single-site rotations expand simply

$$e^{i\beta s_r^y} = \sum_{n=0}^{\infty} \frac{(i\beta)^n}{n!}(s_r^y)^n = \cos\frac{\beta}{2} + (s_r^+ - s_r^-)\sin\frac{\beta}{2}. \tag{A.6}$$

Then the matrix elements on the right of (A.5) are expanded into 1- and 2-site products

$$\begin{aligned}&\langle 0|\boldsymbol{s}_p \cdot \boldsymbol{s}_q \prod_r e^{i\beta s_r^y}|0\rangle \\ &\quad = \langle\sigma(p)\sigma(q)|\boldsymbol{s}_p \cdot \boldsymbol{s}_q\, e^{i\beta s_p^y}\, e^{i\beta s_q^y}|\sigma(p)\sigma(q)\rangle \prod_r^{\neq p,q} \langle\sigma(r)|e^{i\beta s_r^y}|\sigma(r)\rangle,\end{aligned} \tag{A.7}$$

where $\sigma(r)$ is the spin of site r in $|0\rangle$. Substitution of (A.6) into (A.7), then leads to

$$\langle 0|\boldsymbol{s}_p \cdot \boldsymbol{s}_q \prod_r e^{i\beta s_r^y}|0\rangle = -\left(1 - \frac{3}{4}\cos^2\frac{\beta}{2}\right)\left(\cos\frac{\beta}{2}\right)^{N-2} \tag{A.8}$$

and subsequently

$$\langle\Phi|H|\Phi\rangle = -JNz\int_0^{\pi} \sin\beta \cdot \left(1 - \frac{3}{4}\cos^2\frac{\beta}{2}\right)\left(\cos\frac{\beta}{2}\right)^{N-2} d\beta. \tag{A.9}$$

A similar development of the overlap yields

$$\langle\Phi|\Phi\rangle = \tfrac{1}{2}\int_0^{\pi} \sin\beta \cdot \left(\cos\frac{\beta}{2}\right)^{N} d\beta. \tag{A.10}$$

The integrals in (A.9) and (A.10) are readily evaluated by taking $\cos^2(\beta/2) = (1+\cos\beta)/2$ and changing the integration variable to $u = 1+\cos\beta$. The final result is as quoted in (7).

Appendix B: antiferromagnetic spin-wave theory

The approach is a standard [7] extension of Holstein and Primakoff's [22] ferromagnetic spin-wave theory. A transformation is made

$$s_p^{\pm} \equiv \begin{cases} a_p^{\pm}\sqrt{1 - a_p^+ a_p^-}, & p \in A \\ \sqrt{1 - b_p^+ b_p^-}\, b_p^{\pm}, & p \in B, \end{cases} \tag{B.1}$$

with a_p^+, a_p^-, b_p^+, b_p^- being Boson creation and annihilation operators. The spin $\sigma(r)$ for site r in $|0\rangle$ is the 0-Boson state for mode r, while $-\sigma(r)$ is the 1-Boson

state, so that the Néel state is the vacuum. Higher Boson occupation numbers are unphysical, with only the (block-diagonalized) representation of the spin operators of (B1) (and of the associated H) on the subspace of 0- and 1-Boson modes corresponding to the physical situation. The standard approach to expand the square roots of (B1) in powers of the number operators, followed by truncation, then generally leads to (nonvariational) approximations which admix the undesired nonphysical portion of the space. Such truncation of H at terms no more than quadratic in the Boson operators, yields a form that is diagonalizable by the usual Bogoliubov-type canonical transformations. The resulting ground-state energy estimate is [7] (allowing for complex γ_k)

$$E_{\text{Afsw}} = \left\{ -\frac{3}{4}z + \frac{1}{N}\sum_{k} \sqrt{z^2 - |\gamma_k|^2} \right\} JN, \tag{B.2}$$

where the k are wavevectors associated to just one of the two (assumed equivalent) sublattices and where

$$\gamma_k \equiv \sum_{\delta} e^{ik\cdot\delta} \tag{B.3}$$

with the δ being the nearest-neighbor displacement vectors for the chosen sublattice. For the cyclic-chain case (B2) reduces to

$$\frac{E_{\text{Afsw}}}{JN} = \begin{cases} -\frac{3}{2} + \frac{4}{N}\operatorname{ctn}\frac{2\pi}{N}, & N = 4, 8, 12, \ldots \\ -\frac{3}{2} + \frac{2}{N}\operatorname{ctn}\frac{\pi}{N}, & N = 6, 10, 14, 18, \ldots . \end{cases} \tag{B.4}$$

For the $N \to \infty$ limit of the graphite lattice (B.2) reduces to

$$\frac{E_{\text{Afsw}}}{JN} = -\frac{9}{4} + \frac{\sqrt{2}}{4\pi^2}\int_{-\pi}^{\pi}\int_{-\pi}^{\pi} \sqrt{1 - \cos(\alpha+\beta)\cdot\cos\alpha\cdot\cos\beta}\, d\alpha\, d\beta, \tag{B.5}$$

which was evaluated numerically.

Appendix C: real-space renormalization

Real-space renormalization techniques very much like that reviewed by Caspers [18] for Heisenberg models are briefly described here. One starts with a partitioning of the system lattice into equivalent clusters. The collection of isolated clusters are to be considered as a zero-order system and the remaining intercluster interactions treated as a perturbation. Treatment of the zero-order ground-state eigenspace through first-order of (generally degenerate) perturbation theory yields an upper bound to the perturbed ground-state energy. Further the resulting effective Hamiltonian defined just on this zero-order eigenspace typically has an especially simple form very like that of the initial Heiseberg model. This similarity can be especially pronounced if, when the clusters are contracted to super-sites, the resulting inter-super-site interactions form a lattice of the same type as the original.

As a first case on the graphite lattice we consider the 4-site clusters of Fig. 3. In this renormalization process four $(n-1)$th stage clusters combine to form an nth stage cluster, the overall lattice at any stage being that of graphite. For example Fig. 5 illustrates an (n)th stage cluster in terms of $(n-1)$th stage clusters. The Hamiltonian for an nth stage cluster is

$$H_n = 4^n \varepsilon_{n-1} + 2J_n(\boldsymbol{s}_a \cdot \boldsymbol{s}_b + \boldsymbol{s}_a \cdot \boldsymbol{s}_c + \boldsymbol{s}_a \cdot \boldsymbol{s}_d), \tag{C.1}$$

where each of the $(n-1)$th stage clusters (numbered in accordance with the pattern of Fig. 3) have 4^n sites, a per-site energy of ε_{n-1}, and an exchange-coupling parameter J_n to other $(n-1)$th stage clusters. Coupling spins $\boldsymbol{s}_b$, $\boldsymbol{s}_c$, and $\boldsymbol{s}_d$ together to $\boldsymbol{s}_{(a)}$, one obtains the interaction of (C.1) as $\boldsymbol{s}_a \cdot \boldsymbol{s}_{(a)}$. Thence the eigenvalues of overall spin S are seen to be

$$E_n(S, s_{(a)}) = 4^n \varepsilon_{n-1} + J_n\{S(S+1) - S_{n-1}(S_{n-1}+1) - s_{(a)}(s_{(a)}+1)\}, \tag{C.2}$$

where S_{n-1} is the ground-state spin for an $(n-1)$th stage cluster. Now the nth-stage ground state may be verified to have $s_{(a)} = 3S_{n-1}$, overall spin

$$S_n = S = 2S_{n-1} = 2^{n-1} \tag{C.3}$$

and overall energy

$$E_n(2S_{n-1}, 3S_{n-1}) = 4^n \varepsilon_{n-1} - 2S_{n-1}(3S_{n-1}+1)J_n. \tag{C.4}$$

Recurrence relations for the J_n result from matrix element analysis. Let $|A; M\rangle$ be a ground state (with z-component of spin M) for an nth stage cluster A. Then

$$\langle AM_A \times BM_B | 2J_n \boldsymbol{s}_e \cdot \boldsymbol{s}_f | AM'_A \times BM'_B \rangle$$
$$= 2J_n \sum_{\mu} \langle A; M_A | s_e^{\mu} | A; M'_A \rangle \langle B; M_B | s_f^{\mu} | B; M'_B \rangle, \tag{C.5}$$

where $\boldsymbol{s}_e$ and $\boldsymbol{s}_f$ are spins for $(n-1)$th stage clusters in A and B, respectively. But the Wigner-Eckart theorem [23] may be applied to give, e.g.,

$$\langle A; M_A | s_e^{\mu} | A; M'_A \rangle = \gamma_n \langle A; M_A | s_A^{\mu} | A; M'_A \rangle, \tag{C.6}$$

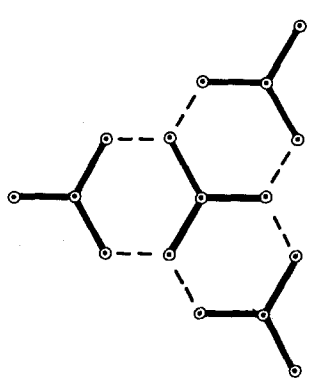

Fig. 5. An $(n+1)$th stage cluster built-up from four nth stage clusters each of which in turn is built-up from four $(n-1)$th stage clusters each represented by a circle here

where γ_n is an appropriate ratio of "reduced matrix elements". This is given as

$$\gamma_n = \frac{\langle A; M|s_e^z|A; M\rangle}{\langle A; M|S_A^z|A; M\rangle} = \frac{1}{3M}\langle A; M|s_{(a)}^z|A; M\rangle \tag{C.7}$$

and this last matrix element may, for instance, be evaluated by Eq. (7) on p. 61 (Sect. 8.3) of Condon and Shortley's text [23] to give

$$\gamma_n = \frac{1}{3}\frac{3S_{n-1}+1}{2S_{n-1}+1}. \tag{C.8}$$

Thus

$$J_{n+1} = \gamma_n^2 J_n \tag{C.9}$$

and the final result for the energy per site is

$$\varepsilon_n = \varepsilon_{n-1} - 4^{-n}\cdot 2^{n-1}(3\cdot 2^{n-2}+1)\prod_{m=1}^{n-1}\gamma_m^2 J, \tag{C.10}$$

where $\varepsilon_1 = -5J/8$. For the lattice we take the limit as $n\to\infty$.

As a second case we consider 7-site clusters, two of which are shown in Fig. 6. In this situation both the lattice and the cluster spin remain the same upon renormalization. The development still parallels the 4-site case, and key use is again made of the Wigner-Eckart theorem. The energy per site that results is

$$\varepsilon_\infty = \frac{E_1}{7-\gamma_b^2-\gamma_e^2}, \tag{C.11}$$

where E_1 is the energy of a single first-stage cluster, and the γ_b, γ_e are reduced marix element ratios for sites b, e of Fig. 3. They are the same at every stage,

$$\gamma_i = \tfrac{4}{3}\langle A; M|\boldsymbol{s}_A\cdot\boldsymbol{s}_i|A; M\rangle. \tag{C.12}$$

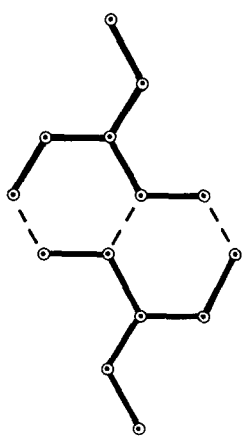

Fig. 6. Two 7-site clusters illustrating the three intercluster couplings, which (with reference to the labelling of Fig. 3) may be taken to be between two e-type, two b-type, and two e-type sites

The quantities E_1 and γ_i were evaluated numerically from a computer diagonalization of the basic 7-site Hamiltonian.

Appendix D: fragments, bounds, and long-range order

First consider a spin-singlet fragment which when iterated exactly covers Γ. Letting $|A\rangle$ and $|B\rangle$ be two such disjoint fragments containing sites i and j, one may readily verify

$$\langle A0 \times B0 | \boldsymbol{s}_i \cdot \boldsymbol{s}_j | A0 \times B0 \rangle = 0 \tag{D.1}$$

using either the Wigner–Eckart theorem (as in Appendix C) or Pauling [24] "island counting" rules. As a consequence the energy for a wavefunction which is a product of those for such singlet fragments is simply a sum of the fragment energies. This approach using singlet fragments may also be viewed as a real-space renormalization-group approach where the Hamiltonian renormalizes to a scalar at the first step.

Next the energies per site as calculated for such first-order renormalization group related approaches provide upper bounds to the energy per site of the system Γ. For the case of singlet fragments this is clear since the energy is calculated in the Rayleigh–Ritz functional form. For the renormalization-group approach of Appendix C it is also true because first-order degenerate perturbation Hamiltonians if solved exactly also yield a Rayleigh–Ritz result.

It may also be noted that wavefunctions which are products of spin-singlet fragments display long-range spin-pairing order, perhaps somewhat diminished from that of the resonance-theory wavefunctions. This is most readily seen for an infinite (cyclic) chain, where the singlet fragments are even-length subchains, so that each contributing Rumer (covalent VB) structure has a limited finite length for spin pairings. But as described elsewhere [4] a finite-range cut-off for such spin-pairings leads to long-range spin-pairing order. Related arguments for benzenoid Γ are indicated in [5] when soliton-antisoliton vacuum fluctuations are discussed.

References

1. See, e.g., Wheland GW (1955) Resonance in organic chemistry. John Wiley and Sons, New York
2. See, e.g., Mattis DC (1965) The theory of magnetism. Harper and Row, New York
3. Smart JS (1966) Effective field theories of magnetism. WB Co., Philadelphia
4. (a) Klein DJ, Garciá-Bach MA (1979) Phys Rev B19:877 (b) Klein DJ (1979) Int J Quantum Chem 13S:293
5. Hite GE, Metropolous A, Klein DJ, Schmalz TG, Seitz WA: preceding paper
6. (a) Seitz WA, Klein DJ, Schmalz TG, Garciá-Bach MA, (1985) Chem Phys Lett 115:139 (b) Klein DJ, Schmalz TG, Metropoulos A, Hite GE, Seitz WA (1985) Chem Phys Lett 120:367
7. See, e.g., Jones W, March NH (1973) Theoretical solid state physics, vol 1, chap 4.4. Wiley-Interscience, New York
8. (a) Hartmann H (1947) Z Naturforsch 2A:259 (b) Davis HL (1960) Phys Rev 120:787
9. Pauling L (1933) The nature of the chemical bond. Cornell University Press, Ithaca

10. Swinbourne-Sheldrake R, Herndon WC, Gutman I (1975) Tetrahedron Lett 755
11. Lieb EH, Mattis DC (1962) J Math Phys 3:749
12. At least this is true for $S/N \sim 0$. For spin projections with spin $S/N > 0$ (for large N systems) the energy can be raised by a size extensive amount. See Klein DJ, Garcia-Bach MA (1977) Int J Quantum Chem 11:291
13. Alexander SA, Schmalz TG, J Am Chem Soc (submitted)
14. Ramasesha S, Soos ZG (1984) Int J Quantum Chem 25:1003
15. Marshall W (1955) Proc Roy Soc A232:69
16. (a) Fisher JC (1959) J Phys Chem Solids 10:44; (b) Qguchi T (1963) J Phys Chem Solids 24:1049
17. See, e.g., (a) Garciá-Bach MA, Klein DJ (1977) Int J Quantum Chem 11:273; (b) van den Broek WJ (1985) Ground-state properties of antiferromagnetic systems. Proefschrift at technische Hogeschool Twente
18. Caspers WJ (1980) Phys Rep 63:223
19. (a) Anderson PW (1975) Mat Res Bull 8:153; (b) Fazekas P, Anderson PW (1974) Phil Mag 30:423; (c) Fazekas P (1980) J Phys C13:L209
20. Here "benzenoid" or "aromatic" systems might be defined as systems none of whose conjugated circuits appearing in any Kekulé structure are devisable by 4; This includes subsections of the honeycomb lattice
21. Klein DJ (1982) J Phys 15A:661
22. Holstein T, Primakoff H (1940) Phys Rev 58:1098
23. Condon EU, Shortley SH (1951) The theory of atomic spectra. University Press, Cambridge
24. Pauling L (1933) J Chem Phys 1:280